Characterization of stationary states in random walks with stochastic resetting

Vicenç Méndez and Daniel Campos

Grup de Física Estadística. Departament de Física. Facultat de Ciències. Edifici Cc. Universitat Autònoma de Barcelona, 08193 Bellaterra (Barcelona) Spain

(Received 20 October 2015; revised manuscript received 22 December 2015; published 2 February 2016)

It is known that introducing a stochastic resetting in a random-walk process can lead to the emergence of a stationary state. Here we study this point from a general perspective through the derivation and analysis of mesoscopic (continuous-time random walk) equations for both jump and velocity models with stochastic resetting. In the case of jump models it is shown that *stationary states* emerge for any shape of the waiting-time and jump length distributions. The existence of such state entails the saturation of the mean square displacement to an universal value that depends on the second moment of the jump distribution and the resetting probability. The transient dynamics towards the stationary state depends on how the waiting time probability density function decays with time. If the moments of the jump distribution are finite then the tail of the stationary distributions is universally exponential, but for Lévy flights these tails decay as a power law whose exponent coincides with that from the jump distribution. For velocity models we observe that the stationary state emerges only if the distribution of flight durations has finite moments of lower order; otherwise, as occurs for Lévy walks, the stationary state does not exist, and the mean square displacement grows ballistically or superdiffusively, depending on the specific shape of the distribution of movement durations.

DOI: 10.1103/PhysRevE.93.022106

I. INTRODUCTION

Random walks represent a recurrent tool to explore transport in systems subject to noise, fluctuations, and/or uncertainty. In many applications, such walks can be interrupted (either by the moving particle or individual itself or by external forces) in such a way that the walker is brought back to its initial position and allowed to continue its movement from there newly. If this process is also driven by some noisy or fluctuating force we term it stochastic resetting. For example, in many spatial searches a natural tendency of living organisms is to return to the origin and start the search again after an unsuccessful excursion [1]. This is meaningful for example in foraging or other movement processes in animals which are often constrained by the presence of predators or other threats that can lead to the interruption of the movement as a risk-averse strategy or as a form of sheltering [2]. In a different context, stochastic resetting can be useful to describe information spreading [3] or searches through graphs [4], particularly in Internet or other communication networks. While the applicability of resetting models to such real situations is still elusive and no direct comparison to real data, as far as we know, has been provided, the interest for the theoretical properties of the models is continuously expanding. In most of the cases, the focus is put in understanding the effects of stochastic resetting as a mechanism to enhance search efficiency (measured as the mean first passage time to a given target) under uninformed (random) search scenarios; an idea which has been explored in a formal way both for the Brownian motion case [5] and for exponential [6] and Lévy flights [7].

Another interest of resetting is in the dramatic effects it has over the stationary properties of transport processes. In Refs. [5,8,9] the authors found how Brownian particles subject to stochastic resetting evolve towards a nonequilibrium stationary state different from a Gaussian distribution due to the nonvanishing flux introduced by the resetting, which violates the detailed balance condition. However, to date few attention has been put in studying the general conditions under which this nonequilibrium stationary state is expected to emerge. Moreover, some additional magnitudes which are typically of interest in random-walk processes, as the mean square displacement (MSD) (whose behavior can also give significant hints about the dynamics in the stationary regime), have not been computed for these situations. In this work we try to fill this gap by proposing a mesoscopic framework (based on the continuous-time random walk scheme) which includes both jump and velocity models. It is confirmed in general that the presence of the stationary state implies that the MSD grows monotonically towards a saturating value that equals the second moment of the distribution at the stationary state. If such saturating value does not exist, this is a signature that the stationary state is never reached (we will see this is the case for Lévy walks and similar processes). The relaxation dynamics towards this value depends on the corresponding waiting-time distribution. We consider several different situations with Markovian and non-Markovian distributions in both jump and velocity models. Specifically we review and extend here the results for the Lévy flight case (which has already been discussed in Refs. [5,7]), and we study for the first time the case of Lévy walks as a particular case of a velocity model.

II. RESETTING CTRW

We consider a unidimensional random-walk process starting from $x = 0$ such that the walker has the possibility to reset its position to that origin whenever a single displacement is completed. We will denote by $X_1, X_2, \dots$ the successive positions of the particle after the first, second, etc. event, where each event can be either a displacement or a reset. If we define r as the resetting probability, then the position X_{i+1} of the particle after the $(i+1)$-th event is chosen as $X_{i+1} = 0$ with probability r, provided the previous (ith) event was not a reset. Otherwise, we choose $X_{i+1} = X_i + Z_i$, where the displacement length Z_i is a random variable drawn from the probability distribution function (PDF) $\Phi(x)$. We term this resetting mechanism as being *subordinated to displacements* [6] since the statistics of the displacements determines in part the rate at which resetting will occur. In order to take into account how different motion patterns affect the emergence of a stationary state in this system, we compare here jump and velocity models. In the former, "movements" consist of instantaneous jumps which are separated by random waiting times or pauses between them. In the latter these events consist of displacements done with finite speed v_0, so the distance traveled during one of these events and the movement duration are coupled variables.

Denote by $j(x,t)$ the density of particles starting a displacement from x at time t if it was initially at $x = 0$. A mesoscopic balance equation for $j(x,t)$ can be written then as

$$j(x,t) = \delta(t)\delta(x) + (1-r)\int_0^t dt' \int_{-\infty}^{\infty} dx' \Psi(x',t') j(x-x',t-t') + r\delta(x)\int_0^t dt' \int_{-\infty}^{\infty} dx \varphi(t') j(x,t-t'). \tag{1}$$

Here $\Psi(x,t)$ is the joint probability of performing a displacement of length x during time t and the PDF for waiting times (in the jump's model) or movement duration (in the velocity's model) is given by $\varphi(t) = \int \Psi(x,t)\,dx$. So the last term in (1) implicitly indicates that the resetting can only occur after a movement event has been completed.

We define the Fourier-Laplace transform of an arbitrary function $g(x,t)$ as

$$g(k,s) = \int_0^{\infty} dt e^{-st} \int_{-\infty}^{\infty} dx e^{-ikx} g(x,t). \tag{2}$$

Transforming Eq. (1) to the Fourier-Laplace space we obtain

$$j(k,s) = \left[1 + r\frac{\varphi(s)}{1-\varphi(s)}\right]\frac{1}{1-(1-r)\Psi(k,s)}. \tag{3}$$

The details of the derivation of Eq. (3) can be found in the Appendix.

III. JUMP MODEL

When displacement distances and waiting times are considered uncoupled random variables we can write $\Psi(x,t) = \Phi(x)\varphi(t)$. In this particular situation, from Eq. (3), the flux density of particles takes the form

$$j(k,s) = \left[\frac{1}{\varphi(s)} + \frac{r}{1-\varphi(s)}\right]\frac{1}{\varphi(s)^{-1} - (1-r)\Phi(k)}. \tag{4}$$

The density of particles located at x at time t is given by

$$P(x,t) = \int_0^t dt' \varphi^*(t') j(x,t-t'). \tag{5}$$

This accounts for particles jumping to point x at time $t - t'$ provided no jumps occur during the remaining time t'. The function $\varphi^*(t) = \int_t^{\infty} dt' \varphi(t')$ is the survival probability of $\varphi(t)$, i.e., the probability for the particle not to jump away until time t.

Making use of the Fourier-Laplace transform defined in Eq. (2), Eq. (5) becomes

$$P(k,s) = \frac{1}{s}\frac{\varphi(s)^{-1} - 1 + r}{\varphi(s)^{-1} - (1-r)\Phi(k)}, \tag{6}$$

where we have employed Eq. (4).

A. Relaxation towards the stationary state

In the large time limit $t \to \infty$ (which is equivalent to the limit $s \to 0$ in the Laplace space) a waiting time PDF with finite first moment $\langle t \rangle$ (mean waiting time) can be expanded through $\varphi(s) \simeq 1 - s\langle t \rangle$, and so Eq. (6) reads

$$P(k,s) \simeq \frac{1}{s}\frac{r + s\langle t \rangle}{1 + s\langle t \rangle - (1-r)\Phi(k)}. \tag{7}$$

This can be inverted back to the real space in time to obtain

$$P(k,t) \simeq P_s(k)\left[1 + \frac{1-r}{r}\frac{1-\Phi(k)}{1-(1-r)\Phi(k)} e^{[1-(1-r)\Phi(k)]\frac{t}{\langle t \rangle}}\right]. \tag{8}$$

This reflects a temporal exponential relaxation towards the stationary state

$$P_s(k) = \frac{r}{1-(1-r)\Phi(k)} \tag{9}$$

since $0 < \Phi(k) \leqslant 1$ in the Fourier space, or towards

$$P_s(x) = \frac{r}{\pi}\int_0^{\infty} \frac{\cos(kx)\,dk}{1-(1-r)\Phi(k)} = r\delta(x) + \frac{r(1-r)}{\pi}\int_0^{\infty} \frac{\Phi(k)\cos(kx)\,dk}{1-(1-r)\Phi(k)} \tag{10}$$

in the real space. This is the nonequilibrium stationary state distribution for any symmetric jump PDF $\Phi(x)$ that is formed and sustained as a result of the permanent influx of particles to the origin due to the resetting process.

Let us deal now with the case where $\varphi(t)$ lacks finite moments. Consider the power-law PDF for waiting times that in the Laplace space reads $\varphi(s) = [1 + (s\tau)^{\gamma}]^{-1}$ with $0 < \gamma < 1$. Inserting this into Eq. (6) we get

$$P(k,s) = \frac{1}{s}\frac{[r + (s\tau)^{\gamma}]}{1 + (s\tau)^{\gamma} - \Phi(k)(1-r)}. \tag{11}$$

This equation can be inverted exactly by Laplace as follows:

$$P(k,t) = \frac{r}{\tau^{\gamma}} t^{\gamma} E_{\gamma,\gamma+1}\left[-a(k)\frac{t^{\gamma}}{\tau^{\gamma}}\right] + E_{\gamma}\left[-a(k)\frac{t^{\gamma}}{\tau^{\gamma}}\right], \tag{12}$$

where $E_{\gamma}(z)$ and $E_{\gamma,\gamma+1}(z)$ are Mittag-Leffler and Generalized Mittag-Leffler functions, respectively, and $a(k) = 1 - (1-r)\Phi(k)$. Making use of the asymptotic expansions

$$E_{\gamma}(z) = -\frac{1}{z\Gamma(1-\gamma)} + O(z^{-2}), E_{\gamma,\gamma+1}(z) = \frac{E_{\gamma}(z) - 1}{z} = -z^{-1} + O(z^{-2}) \tag{13}$$

as $|z| \to \infty$ if $0 < \gamma < 1$, we can expand Eq. (12) for $t \to \infty$ to get

$$P(k,t) \simeq \frac{r}{a(k)}\left[1 + \frac{1}{r}\left(\frac{\tau}{t}\right)^{\gamma} + \cdots\right] \tag{14}$$

so that the relaxation towards the stationary distribution follows a power-law decay.

B. Properties of the stationary state

The shape of the stationary state given by (10) can only be found exactly for some particular cases. For example, consider the exponential jump PDF

$$\Phi(x) = \frac{1}{2\lambda}\exp(-|x|/\lambda) \tag{15}$$

with $\lambda > 0$ (also known as Laplace kernel). Its Fourier transform reads $\Phi(k) = (1 + k^2\lambda^2)^{-1}$. Then from (10) we have that the stationary state reads

$$P_s(x) = r\delta(x) + \frac{(1-r)\sqrt{r}}{2\lambda}e^{-|x|\frac{\sqrt{r}}{\lambda}},$$

an expression similar to that previously obtained in Ref. [5].

Let us inspect now the form of the stationary distribution from a more general perspective. First, we consider the diffusive limit, i.e., expand the jumps PDF $\Phi(x)$ up to the second moment $\Phi(k) \simeq 1 - \sigma^2 k^2/2$ as $\sigma k \ll 1$. In this case Eq. (10) reduces to

$$P_s(x) \simeq \frac{1}{2\sigma}\sqrt{\frac{2r}{1-r}}e^{-|x|\frac{1}{\sigma}\sqrt{\frac{2r}{1-r}}}, \text{ for } |x| \gg \sigma. \tag{16}$$

Therefore, all jump distance PDFs with finite moments have a stationary state decaying as in (16), where σ^2 is its second moment, $\sigma^2 = \int x^2\Phi(x)\,dx$. It has been found recently [9] how such a stationary state is transiently followed in the case of Brownian motion by a still further region (for $|x| \leqslant \sqrt{4Drt}$, with D the diffusion coefficient of the Brownian walker) which includes those particles that have not experienced yet the effect of resetting, and that becomes eventually negligible in the large-time regime.

Besides the asymptotic behavior, note that the shape of the stationary state close to $x = 0$ can also be approximated by expanding the $\cos(kx)$ in power series in Eq. (10). By doing that we have

$$P_s(x) \simeq a_0 - a_1 x^2, \quad \text{for } x \to 0, \tag{17}$$

where

$$a_0 = r\delta(x) + \frac{r(1-r)}{\pi}\int_0^{\infty}\frac{\Phi(k)\,dk}{1-(1-r)\Phi(k)},$$
$$a_1 = \frac{r(1-r)}{2\pi}\int_0^{\infty}\frac{k^2\Phi(k)\,dk}{1-(1-r)\Phi(k)}. \tag{18}$$

In Fig. 1 we plot the stationary state reached when the jump PDF obeys a Gaussian distribution $\Phi(x) = [\sigma\sqrt{2\pi}]^{-1}\exp(-x^2/2\sigma^2)$ after extracting the term $r\delta(x)$. It is seen how the stationary distribution is more peaked around $x = 0$ as r tends to 1, i.e., as the probability of reseting increases. The lines in the tails correspond to the exponential decay predicted by Eq. (16). Likewise, the lines of the central part correspond to the approximated solution given in Eq. (17).

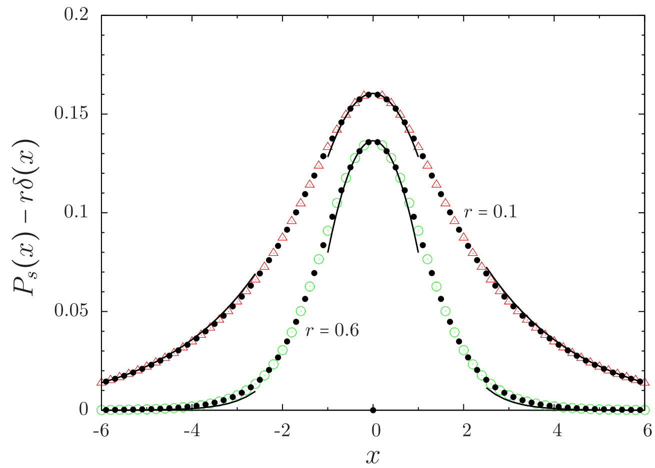

FIG. 1. $P_s(x)$ with a $\Phi(x)$ given by the Gaussian PDF for different values of the probability of resetting r. The results calculated from Eq. (10) have been drawn with symbols $\sigma = 1$. Stochastic simulations directly performed for Eqs. (1) and (5) are shown with filled circles exhibiting an excellent agreement. The solid curves indicate the approximations to the tails and the central part of $P_s(x)$.

We consider now the case of a Lévy distribution for jumps for which $\Phi(k) = e^{-\sigma^{\mu}|k|^{\mu}}$, with $1 \leqslant \mu \leqslant 2$. Since $0 < \Phi(k) < 1$ then we can convert the right-hand side of (9) into the sum

$$P_s(k) = r\sum_{j=0}^{\infty}(1-r)^j\Phi(k)^j = r\sum_{j=0}^{\infty}(1-r)^j e^{-j\sigma^{\mu}|k|^{\mu}}$$
$$= \frac{r}{\sigma}\sum_{j=0}^{\infty}(1-r)^j j^{-1/\mu}L_{\mu}\left[\frac{|x|}{\sigma j^{1/\mu}}\right], \tag{19}$$

where $L_{\mu}[x]$ is the normalized Lévy density defined by

$$L_{\mu}\left[\frac{|x|}{\sigma}\right] = \sigma\int_{-\infty}^{\infty}e^{-ikx-\sigma^{\mu}|k|^{\mu}}\,dx.$$

Expression (19) can be written in terms of Fox functions $H_{n,m}^{p,q}(z)$ [10] in the form

$$P_s(x) = \frac{r\pi}{\mu|x|}$$
$$\times\sum_{j=0}^{\infty}(1-r)^j H_{2,2}^{1,1}\left[\frac{|x|}{\sigma}j^{\frac{-1}{\mu}}\middle|\begin{matrix}(1,\frac{1}{\mu}), & (1,\frac{1}{2})\\ (1,1), & (1,\frac{1}{2})\end{matrix}\right]$$
$$= \frac{r\mu}{|x|}\sum_{n=0}^{\infty}a(r,n,\mu)\left(\frac{\sigma}{|x|}\right)^{n\mu} \tag{20}$$

for $|x| \gg \sigma$, where

$$a(r,n,\mu) \equiv \frac{(-1)^{n+1}\Gamma(n\mu)}{(n-1)!}\sin\left(\frac{n\mu\pi}{2}\right)\sum_{j=1}^{\infty}j^n(1-r)^j.$$

The tail of this stationary distribution behaves as

$$P_s(x) \simeq \frac{(1-r)\Gamma(\mu)\sin(\pi\mu/2)}{r}\frac{\sigma^{\mu}}{|x|^{\mu+1}}, \tag{21}$$

just as the Lévy distribution in the real space. So, unlike the case where the jump PDF has finite moments the tail decays

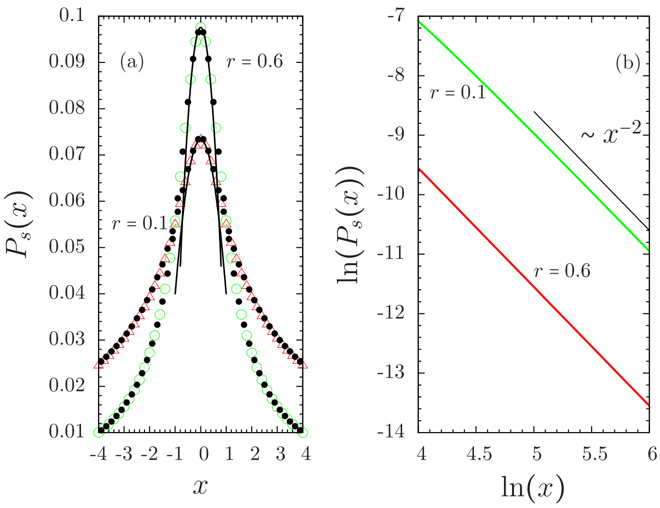

FIG. 2. (a) $P_s(x)$ (symbols) for the Cauchy jump PDF for different values of the probability of resetting r. The symbols correspond to the solutions calculated from Eq. (10) taking $a = 1$. Stochastic simulations directly performed for Eqs. (1) and (5) are shown with filled circles exhibiting an excellent agreement. (b) Log-log plot for $P_s(x)$ for the Cauchy jump PDF for different values of the probability of resetting r. The solid curves have been calculated from Eq. (10) taking $a = 1$.

as that of the stationary distribution. In Fig. 2 we provide the same plot as in Fig. 1 but now for a Cauchy distribution

$$\Phi(x) = \frac{a/\pi}{x^2 + a^2},$$

which corresponds to a Lévy distribution with $\mu = 1$ and $\sigma = a$.

The lines showed in the Fig. 2(a) correspond to the approximations for small x prescribed in Eq. (17). Solid circles correspond to numerical solutions Again, the stationary distribution is more peaked around $x = 0$ for higher values of r and the tails decay heavily. To study more accurately the behavior of the tails we show in Fig. 2(b) the tails for the same curves in a log-log scale.

The flux density $j(x,t)$ also decays towards a stationary value $j_s(x)$ in the limit $t \to \infty$ but when the waiting time PDF has finite moments only. From Eq. (3), and proceeding in the same way as we have done for $P(x,t)$, the stationary flux density reads

$$j_s(x) = \frac{r}{2\pi \langle t \rangle} \int_{-\infty}^{\infty} \frac{e^{ikx}\, dk}{1 - (1-r)\Phi(k)} = \frac{P_s(x)}{\langle t \rangle}. \quad (22)$$

If $\Phi(x)$ is exponentially distributed as in Eq. (15), then from (22) we find the exact solution

$$j_s(x) = \frac{(1-r)\sqrt{r}}{2\langle t \rangle \lambda} e^{-\frac{|x|}{\lambda}\sqrt{r}} + \frac{r}{\langle t \rangle}\delta(x). \quad (23)$$

Additionally, we consider again the case of a Lévy distribution for the jump PDF to compute the flux density at the stationary state

$$j_s(x) = \frac{r}{\sigma \langle t \rangle} \sum_{j=0}^{\infty} \frac{(1-r)^j}{j^{1/\mu}} L_\mu\left[\frac{|x|}{\sigma j^{1/\mu}}\right]. \quad (24)$$

Note that in all cases the flux density diverges at $x = 0$ due to the effect of incoming particles from resetting, except trivially for $r = 0$ (this is, when we remove resetting).

C. MSD

To compute the MSD we have to assume that $\Phi(x)$ has finite moments. By using Eq. (6) we have

$$\langle x^2(s) \rangle = -[\partial_{kk} P(k,s)]_{k=0} = \frac{(1-r)\langle l^2 \rangle}{s[\varphi(s)^{-1} - 1 + r]}, \quad (25)$$

where $\langle l^2 \rangle$ is the second moment of $\Phi(x)$, i.e., $\langle l^2 \rangle = -[\Phi''(k)]_{k=0}$. If we consider the Markovian case where the waiting-time PDF is exponentially distributed, i.e., $\varphi(t) = \tau^{-1} e^{-t/\tau}$ (or, equivalently in Laplace space $\varphi(s) = (1 + s\tau)^{-1}$), then employing Eq. (25) it follows

$$\langle x^2(t) \rangle = \frac{(1-r)\langle l^2 \rangle}{r}(1 - e^{-rt/\tau}). \quad (26)$$

This shows an exponential convergence to the asymptotic value $(1-r)\langle l^2 \rangle / r$ with a characteristic relaxation time τ/r.

Let us now consider the non-Markovian case where the waiting-time PDF decays as a power law in time. In the large time limit ($s \to 0$) we consider $\varphi(s) \simeq 1 - (s\tau)^\gamma$. Then (25) reads

$$\langle x^2(t) \rangle = \frac{(1-r)\langle l^2 \rangle}{\tau^\gamma} t^\gamma E_{\gamma,\gamma+1}\left(-\frac{rt^\gamma}{\tau^\gamma}\right)$$
$$= (1-r)\langle l^2 \rangle \left(\frac{t}{\tau}\right)^\gamma \sum_{k=0}^{\infty} \frac{(-1)^k r^k (t/\tau)^{k\gamma}}{\Gamma(k\gamma + \gamma + 1)}. \quad (27)$$

Using the expansion in (13) into (27) leads to the result

$$\langle x^2(\infty) \rangle = \frac{(1-r)\langle l^2 \rangle}{r}, \quad (28)$$

which is independent of the anomalous exponent. This result illustrates that the MSD converges to the above result when $t \to \infty$. On the other hand we can check that this result is

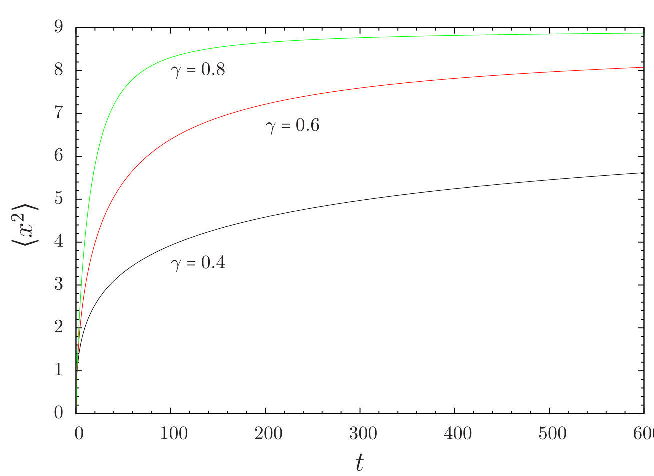

FIG. 3. Plot of the MDS relaxing to the asymptotic value $(1 - r)\langle l^2 \rangle / r$. In this case the jump PDF has finite moments but the waiting-time PDF is a power law, that is, $\langle x^2 \rangle$ is given by Eq. (27). Here $\tau = \langle l^2 \rangle = 1, r = 0.1$.

precisely equal to the second moment of the PDF $P_s(x)$. By its definition, the second moment is

$$\langle x^2(\infty)\rangle = \int_{-\infty}^{\infty} x^2 P_s(x)\,dx = -[\partial_{kk}P(k,\infty)]_{k=0} = \frac{(1-r)\langle l^2\rangle}{r}, \tag{29}$$

where we have used (9). The expression (28) corroborates the result that if $\Phi(x)$ lacks finite moments, then the same happens for the stationary distribution too.

In Fig. 3 we plot the MSD computed from Eq. (27). The relaxation to the asymptotic value given by Eq. (28) follows the power law $t^{-\gamma}$. As a result the relaxation is governed by the value of the exponent γ, as can be checked in Fig. 3 for values from $\gamma = 0.8$ to $\gamma = 0.4$.

IV. VELOCITY MODEL

Note that the resetting mechanism considered here, when applied to velocity models, presents some different properties to those of the jump model (as has been already discussed in [6]). In particular, we find that in the limit $r \to 1$ the dynamics of the walker will consist in "one-flight" excursions followed by resetting events. This looks more realistic that the typical dynamics of random walks with resetting in the jump models or other cases considered before where $r \to 1$ means that the walker remains permanently at $x = 0$ (so no walk or search process exists, actually.)

For the velocity model $\Psi(x,t) = \Phi(x|t)\varphi(t)$ is the joint probability of performing a movement of length $|x| = v_0 t$ with constant speed v_0 during time t. So the quantity $\Phi(x|t)$ is the conditional probability to perform a movement of duration t and with length $v_0 t$. Therefore,

$$\Psi(x,t) = \frac{1}{2}[\delta(x - v_0 t) + \delta(x + v_0 t)]\varphi(t) = \frac{1}{2v_0}\delta\left(t - \frac{|x|}{v_0}\right)\varphi(t), \tag{30}$$

where we consider a probability $1/2$ of moving to the right or to the left. The probability of having completed a movement of distance x is $\Phi(x)$ and can be computed from (30):

$$\Phi(x) = \int_0^{\infty} dt\,\Psi(x,t) = \frac{1}{2v_0}\varphi\left(\frac{|x|}{v_0}\right). \tag{31}$$

In this case the density of particles located at x at time t is given by

$$P(x,t) = \int_0^t dt' \int_{-\infty}^{\infty} dx' \phi(x',t') j(x - x', t - t'), \tag{32}$$

where $\phi(x,t)$ is just the probability that a single displacement has not finished yet after having traveled during a time t and having covered (either to left or right) a distance x. Transforming Eq. (32) by Fourier-Laplace and using Eq. (3) it follows

$$P(k,s) = \left[1 + r\frac{\varphi(s)}{1-\varphi(s)}\right]\frac{\phi(k,s)}{1-(1-r)\Psi(k,s)}. \tag{33}$$

On the other hand,

$$\phi(x,t) \equiv \frac{1}{2}[\delta(x - v_0 t) + \delta(x + v_0 t)]\varphi^*(t) \tag{34}$$

is just the probability that a single movement has not finished yet after having traveled during a time t and having covered (either to left or right) a distance $v_0 t$.

A. Stationary state

To compute the density at the steady state let us take the limit $s \to 0$ in Eq. (33),

$$P(k,s) \simeq \frac{\phi(k,s=0)}{1-(1-r)\Psi(k,s=0)} \lim_{s\to 0}\left[1 + r\frac{\varphi(s)}{1-\varphi(s)}\right] = F(k)\lim_{s\to 0}\left[1 + r\frac{\varphi(s)}{1-\varphi(s)}\right], \tag{35}$$

where we have defined

$$F(k) \equiv \frac{-\mathrm{Im}\,\varphi(ikv_0)}{kv_0[1-(1-r)\mathrm{Re}\,\varphi(ikv_0)]}. \tag{36}$$

Consider the case where the PDF of movement durations has finite moments. In the large time limit we can use the expansion $\varphi(s) \simeq 1 - s\langle t\rangle$, so in this case

$$\lim_{s\to 0}\left[1 + r\frac{\varphi(s)}{1-\varphi(s)}\right] \simeq \frac{r}{\langle t\rangle s} + O(s). \tag{37}$$

Inverting by Fourier (35) and taking into account (36) and (37), the general expression for the stationary state reads

$$P_s(x) = \frac{r}{\pi\langle t\rangle}\int_0^{\infty}\cos(kx)F(k)\,dk. \tag{38}$$

If we want to investigate the tail of the stationary distribution we have to take the large time limit, which in this case is equivalent to the large space limit, since both variables are coupled through v_0. Considering that the PDF of movement durations has finite moments, we have to expand up to second order to capture the leading term in the long time expansion in (36), so that $\varphi(s) \simeq 1 - s\langle t\rangle + s^2\langle t^2\rangle/2$. After inserting this into (36) we get

$$F(k) = \frac{1}{r + \frac{1}{2}(1-r)\langle t^2\rangle k^2 v_0^2}.$$

Introducing this result into (38) we finally obtain

$$P_s(x) \simeq \frac{\sqrt{r}}{\sqrt{2(1-r)\langle t^2\rangle}v_0}\exp\left[-\frac{\sqrt{2r}}{\sqrt{(1-r)\langle t^2\rangle}v_0}|x|\right]. \tag{39}$$

This is the stationary distribution for a velocity model when $|x|$ is large. Unlike the jump model, in the velocity model the $P_s(x)$ depends also on the second moment of the movement duration PDF due to the time-space coupling.

In Fig. 4 we have plotted the exact results given by the Eq. (38) when we make use of the Gamma distribution $\varphi(t) = te^{-t/\tau}/\tau^2$. The lines in the tails correspond to the theoretical asymptotic result predicted by Eq. (39), and the lines at the central part of the distributions are computed through $P_s(x) \simeq a_2 - a_3 x^2$, where

$$a_2 = \frac{r}{\pi\langle t\rangle}\int_0^{\infty}F(k)\,dk, \quad a_3 = \frac{r}{2\pi\langle t\rangle}\int_0^{\infty}k^2F(k)\,dk.$$

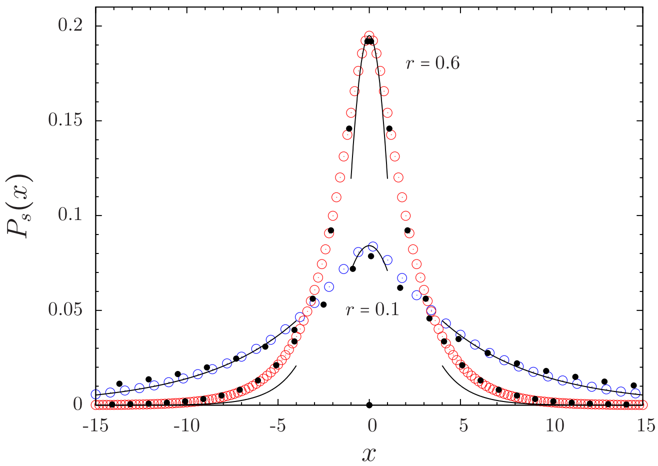

FIG. 4. Stationary distribution (symbols) for a PDF movement durations $\varphi(t) = te^{-t/\tau}/\tau^2$ for different values of r. Stochastic simulations directly performed for Eqs. (1) and (32) are shown with filled circles exhibiting an excellent agreement. The solid curves indicate the approximations to the tails and the central part of $P_s(x)$. $v_0 = \tau = 1$.

This is the highest-order possible approximation to the central part since the integrals

$$\int_0^\infty k^n F(k)\,dk$$

diverge for $n \geqslant 4$. To calculate the coefficients a_2 and a_3 for the case of a Gamma distribution of movement durations in Fig. 4, from (36) we find

$$F(k) = \frac{2\tau}{\left(1 + k^2 v_0^2 \tau^2\right)^2 - (1-r)\left(1 - k^2 v_0^2 \tau^2\right)}.$$

Consider now a non-Markovian example with a power-law PDF of movement durations $\varphi(s) = [1 + (s\tau)^\gamma]^{-1}$. In this case

$$\lim_{s\to 0}\left[1 + r\frac{\varphi(s)}{1-\varphi(s)}\right] \simeq \frac{r}{(s\tau)^\gamma} + O(s).$$

After simplifying (35) we find

$$P(k,s) \simeq \frac{1}{(s\tau)^\gamma}\frac{(k\tau v_0)^{\gamma-1}\sin(\pi\gamma/2)}{1 + \frac{1+r}{r}\cos(\pi\gamma/2)(k\tau v_0)^\gamma + r^{-1}(k\tau v_0)^{2\gamma}}.$$

By inverting the Laplace transform, the factor $(s\tau)^{-\gamma}$ turns into a factor $t^{\gamma-1}$, which tends to 0 as $t \to \infty$ since $0 < \gamma < 1$. Then, when the PDF of movement durations lacks finite moments there is no stationary state and the relaxation to the stationary state $P_s(x) = 0$ follows the power-law decay $t^{\gamma-1}$.

B. MSD

We finally explore the behavior of the MSD when the PDF of movement durations and the PDF of movement distances has or does not have finite moments. Starting from the general expression (33) we find after some calculations

$$\begin{aligned}\langle x^2(s)\rangle &= -[\partial_{kk}P(k,s)]_{k=0}\\ &= v_0^2\left[\frac{(\varphi^*(s))''}{1-\varphi(s)} + \frac{1-r}{s}\frac{\varphi''(s)}{1-(1-r)\varphi(s)}\right], \qquad (40)\end{aligned}$$

where the symbol $''$ means second derivative respect to s. For the case of movement duration PDFs with finite moments we consider the asymptotic expansion $\varphi(s) \simeq 1 - s\langle t\rangle + s^2\langle t^2\rangle/2 - s^3\langle t^3\rangle/6$. Note that in all previous cases we kept a first- or second-order expansion of this PDF in powers of s. However, the existence of a second-order derivative in s in the definition of (40), makes the third-order expansion necessary to capture the highest-order term in the dynamics of the asymptotic value of the MSD. Hence, in the large time limit Eq. (40) reduces to

$$\langle x^2(\infty)\rangle = v_0^2\left(\frac{\langle t^3\rangle}{3\langle t\rangle} + \frac{1-r}{r}\langle t^2\rangle\right). \qquad (41)$$

For the case of the exponential distribution $\varphi(t) = e^{-t/\tau}/\tau$ we have seen that there exists a stationary state so it is expected that the MSD tends to a constant. To find the time dependence of the MSD we make use of (40) and get

$$\langle x^2(t)\rangle = \frac{2v_0^2\tau^2}{r}\left(1 + \frac{re^{-t/\tau} - e^{-rt/\tau}}{1-r}\right). \qquad (42)$$

Performing the limit $t \to \infty$ we find

$$\langle x^2(\infty)\rangle = \frac{2v_0^2\tau^2}{r}.$$

This result equals the second moment of the PDF at the stationary state as already happened in the jump model. Effectively, from (36) we have

$$F(k) = \frac{\tau}{r + k^2 v_0^2 \tau^2}$$

and together with (38)

$$\begin{aligned}\langle x^2(\infty)\rangle &= \int_{-\infty}^{\infty} x^2 P_s(x)\,dx = \frac{\sqrt{r}}{v_0\tau}\int_0^\infty x^2 e^{-x\frac{\sqrt{r}}{v_0\tau}}\,dx\\ &= \frac{2v_0^2\tau^2}{r}. \qquad (43)\end{aligned}$$

Finally, let us consider the case of Lévy walks. They are random walks where the displacements are performed with finite velocity but the jump distribution or the movement duration PDF [lined through Eq. (31)] has tails which decay according to power laws, so higher-order moments are lacking. For example, the PDF $\varphi(s) = [1 + (s\tau)^\gamma]^{-1}$, with $0 \leqslant \gamma \leqslant 1$, lacks all moments including its mean value. If we insert this expression into Eq. (40) we find

$$\langle x^2(t)\rangle = \frac{(2-\gamma)(1-\gamma)}{2}v_0^2 t^2 \quad \text{as} \quad t \to \infty,$$

which corresponds to a ballistic transport regime. This behavior is due to the fact that the probability density of particles $P(x,t)$ is a sandwich between two ballistic peaks located at $x = \pm v_0 t$. Another possibility is to consider $\varphi(s) \simeq 1 - s\langle t\rangle + As^\mu$ with $1 < \mu < 2$. In this case there exists the first moment (but not the second-order or higher). Calculation of the MSD for this case gives from Eq. (40) a superdiffusive behavior

$$\langle x^2(t)\rangle = \frac{(2-\mu)(1-\mu)}{\Gamma(4-\mu)\langle t\rangle}v_0^2 A t^{3-\mu} \quad \text{as} \quad t \to \infty.$$

Again the result does not depend on the probability of resetting explicitly because the asymptotic behavior is dominated by the fraction of particles which have not experienced resetting yet. So in both cases studied (and in general for Lévy walks) we find that there is no stationary state, contrary to what happened for the case of Lévy flights.

V. SUMMARY

In this work we have studied the conditions for the existence of a resetting-induced stationary state and so a saturation value for the MSD in the case of a jump model where jumps distances and waiting times are independent random variables and the walker is submitted to stochastic resetting with probability r. The tail of the stationary distribution is exponential if the jump PDF has finite moments but when the jumps PDF decays as a power law the stationary PDF also decays as a power law with the same exponent. The MSD grows exhibiting an exponential saturation if the waiting time PDF has finite moments or saturates as a power law in time if the waiting time PDF also decays as a power law. The saturating value is always $(1-r)\langle l^2\rangle/r$, where $\langle l^2\rangle$ is the second moment of the jump PDF. In consequence, the finiteness of the second moment (at least for isotropic motion) determines the saturation of the MSD. The situation under advective or biased movement will require further examination and will be the focus of a forthcoming work.

In the velocity model, where the movement of the walker is performed at constant speed v_0, the movement duration PDF defined univocally the jump displacement PDF. When the movement duration PDF has finite moments there is a stationary state with an exponential tail and the MSD saturates always to the value $2v_0^2\tau^2/r$. When it lacks first- or second-order moments, as for the Lévy walks case, there is no stationary state and the MDS grows ballistically or superdiffusively, respectively. This is a consequence of our choice of resetting *subordinated to displacements*; we note that implementing resetting as an independent process of motion (as was done, for example, in Ref. [11] or [6]) then the stationary state will emerge (both for jump and velocity models) whenever the mean time for resetting is finite.

ACKNOWLEDGMENTS

This research has been partially supported by Grants No. FIS 2012-32334 by the Ministerio de Economía y Competitividad and by SGR 2013-00923 by the Generalitat de Catalunya. V.M. also thanks the Isaac Newton Institute for Mathematical Sciences, Cambridge, for support and hospitality during the CGP programme, where part of this work was undertaken.

APPENDIX: DERIVATION OF EQ. (3)

First, we transform Eq. (1) by Fourier-Laplace as has been defined in Eq. (2). However, the third term of the right-hand side of Eq. (1) needs to be transformed by Laplace first to get

$$r\delta(x)\varphi(s)\int_{-\infty}^{\infty} dx j(x,s).$$

Since

$$j(k=0,s)=\int_{-\infty}^{\infty} dx j(x,s)$$

then the Fourier-Laplace transform of Eq. (1) is given by

$$j(k,s)=1+(1-r)\Psi(k,s)j(k,s)+r\varphi(s)j(k=0,s) \quad \text{(A1)}$$

where we have made use of the transform of convolution products. Solving (A1) for $j(k,s)$ we get

$$j(k,s)=\frac{1+r\varphi(s)j(k=0,s)}{1-(1-r)\Psi(k,s)}. \quad \text{(A2)}$$

Evaluating (A2) for $k=0$ and solving for $j(k=0,s)$ we find

$$j(k=0,s)=\frac{1}{1-(1-r)\Psi(k=0,s)-r\varphi(s)}. \quad \text{(A3)}$$

Now we evaluate $\Psi(k=0,s)$. By the definition of Fourier-Laplace transform given in (2),

$$\Psi(k=0,s)=\int_0^{\infty} e^{-st}dt\int_{-\infty}^{\infty} dx\Psi(x,t).$$

Since $\varphi(t)=\int_{-\infty}^{\infty} dx\Psi(x,t)$ we have $\Psi(k=0,s)=\varphi(s)$ and from (A3) we obtain

$$j(k=0,s)=\frac{1}{1-\varphi(s)}.$$

Inserting the above result into (A2) we finally obtain Eq. (3).

[1] D. Campos, F. Bartumeus, V. Méndez, and X. Espadaler, J. Roy. Soc. Interf. **11**, 20130859 (2013).
[2] O. Bénichou, C. Loverdo, M. Moreau, and R. Voituriez, Rev. Mod. Phys. **83**, 81 (2011).
[3] D. Liben-Nowell and J. Kleinberg, Proc. Natl. Acad. Sci. USA **105**, 4633 (2008).
[4] E. Gelenbe, Phys. Rev. E **82**, 061112 (2010).
[5] M. R. Evans and S. N. Majumdar, Phys. Rev. Lett. **106**, 160601 (2011).
[6] D. Campos and V. Méndez, Phys. Rev. E **92**, 062115 (2015).
[7] L. Kusmierz, S. N. Majumdar, S. Sabhapandit, and G. Schehr, Phys. Rev. Lett. **113**, 220602 (2014).
[8] M. R. Evans and S. N. Majumdar, J. Phys. A: Math. Theor. **47**, 285001 (2014).
[9] S. N. Majumdar, S. Sabhapandit, and G. Schehr, Phys. Rev. E **91**, 052131 (2015).
[10] B. J. West, P. Grigolini, R. Metzler, and T. F. Nonnenmacher, Phys. Rev. E **55**, 99 (1997).
[11] M. Montero and J. Villarroel, Phys. Rev. E **87**, 012116 (2013).